PCCP

Cold Collisions of Hot Molecules

Journal:	*Physical Chemistry Chemical Physics*
Manuscript ID	CP-PER-05-2023-002071.R1
Article Type:	Perspective
Date Submitted by the Author:	08-Aug-2023
Complete List of Authors:	Perera, Chatura A.; University of Missouri, Department of Chemistry Amarasinghe, Chandika; University of Missouri, Department of Chemistry Guo, Hua; University of New Mexico, Department of Chemistry Suits, Arthur; University of Missouri, Department of Chemistry

Cold Collisions of Hot Molecules

Chatura A. Perera[1], Chandika Amarasinghe[1,†], Hua Guo[2], and Arthur G. Suits[1,*]

[1]*Department of Chemistry, University of Missouri, Columbia MO 65211, USA*

[2]*Department of Chemistry and Chemical Biology, University of New Mexico, Albuquerque, New Mexico 87131, USA*

Abstract

In this Perspective, we review our recent work on rotationally inelastic collisions of highly vibrationally excited NO molecules prepared in single rotational and parity levels at v=10 using stimulated emission pumping (SEP). This state preparation is employed in a recently developed crossed molecular beam apparatus where two nearly copropagating molecular beams achieve an intersection angle of 4° at the interaction region. This near-copropagating beam geometry of the molecular beams permits very wide tuning of the collision energy, from far above room temperature down to 2 K where we test the theoretical treatment of the attractive part of the potential and the difference potential for the first time. We have obtained differential cross sections for state-to-state collisions of NO(v=10) with Ar and Ne in both spin-orbit manifolds using velocity map imaging. Overall good agreement of the experimental results was seen with quantum mechanical close-coupling calculations done on both coupled-cluster and multi-reference configuration interaction potential energy surfaces. Probing cold collisions of NO carrying a ~2 eV of vibrational excitation allows us to test state-of-the-art theory in this extreme nonequilibrium regime.

[†]Current address: Thermo Fisher Scientific, 355 River Oaks Parkway, San Jose CA 95134, USA
[*]suitsa@missouri.edu

Introduction

Cooling matter to temperatures near absolute zero brings about fascinating questions regarding possible changes in chemical reactivity.[1] How does the low collision energy change the sensitivity to the anisotropy of the potential energy surface (PES)? Or to the attractive vs. repulsive interaction? What happens when the internal degrees of freedom are very far from equilibrium with each other and from the collision event? When might vibrational excitation undermine the accuracy of the theoretical prediction of the outcome? What is the role of resonances and how do they impact the differential cross sections (DCSs) and integral cross sections (ICSs)?[2-4] The familiar notion of reactants passing over an activation barrier to become products can hardly be applied under these conditions, but inelastic processes and barrierless reactions of open shell species remain important. The classical picture of colliding particles useful to guide intuition must be replaced by wave mechanics in cold conditions as we enter a fully quantum realm.[1, 5, 6] In the quantum regime the system of moving and colliding particles must be understood as a superposition of partial waves. This represents the various angular momentum states associated with the relative motion of the colliding species. As we move the system towards the cold and ultracold regimes, interactions can only be explained by a few quantized angular momentum states and ultimately by a single such state. Similarly, at low temperatures only a very few rovibrational states will be populated and finally just a single quantum state as we reach the lowest temperatures. Under these conditions, quantum effects such as collision resonances, quantum tunnelling, stereodynamics, geometric phase effects and long-lived collision complexes are more likely to be observed.[5-8] All these effects are in stark contrast to what is seen at room temperature. These effects can lead to dramatic modulation of reactivity with quantum state or with external fields, yielding new insights into

intermolecular interactions and allowing for manipulation and control of chemical outcomes. In this Perspective, we review our recent work on state-to-state collisions of highly vibrationally excited NO at collision energies above room temperature down to the cold regime. The results are compared to quantum close-coupling calculations on high-level PESs.

Experimental advances in the past decade have opened cold collision dynamics studies to investigation in unprecedented detail. Such studies may broadly be divided into two approaches. The first involves cooling and trapping of molecules or ions. This delivers long interaction times and permits kinetics studies on a timescale of minutes with just a handful of molecules. This is pursued with Coulomb crystals of ions or with neutral molecules prepared from atomic constituents by photoassociation. Studies done on collisions between dipolar bi-alkali molecules in combination with ultracold atoms, for example, have yielded temperatures all the way down to 0.1 mK.[9-12] Furthermore, remarkable advances have been achieved with techniques that use direct slowing or laser cooling of molecules before trapping in the ultracold regime.[13-17] These samples then can be further cooled with optical, evaporative, or sympathetic cooling schemes to obtain sufficient collision cross sections.[18, 19] Molecules in laser-prepared optical lattices manipulated with electric fields or optical tweezers permit extraordinary control over dipole-dipole interactions, and represent an exciting frontier on the physics side of the border between physics and chemistry.

The second broad approach to cold collision studies involves variations on crossed molecular beam methods in which the beams of state-prepared species collide within a well-defined crossing volume.[20, 21] Seeding of the molecules in noble gases and expanding supersonically allows the cooling of the molecules of interest to very low rotational and translational temperatures, and further laser manipulation may be used to select individual quantum states for reaction and

detection. Beams of atoms or molecules may be slowed and manipulated with Stark or Zeeman decelerators to obtain very low collision energies, or, by studying merged beam, intrabeam, or nearly copropagating beam collisions, cold collisions are achieved in the moving frame.

Using the crossed beam technique with a Stark decelerator, inelastic scattering resonances for nitric oxide (NO) with many targets have been successfully studied by van de Meerakker and co-workers with extraordinary control over the collision energy and collision energy spread.[22-25] Resonances in Penning ionization of metastable atoms and few molecules have also been demonstrated using the merged beam technique by the groups of Narevicius and Osterwalder.[26-29] In the merged beam technique, a paramagnetic species (typically a metastable rare gas atom) is guided by a magnetic quadrupole to merge with a target beam for Penning ionization studies. Typically, resonances are seen as the total cross section is monitored as a function of collision energy or also, by further manipulation of the magnetic fields, orbital polarization of the metastable atom. Similarly, one can study intrabeam collisions at very low energies simply by using a laser to prepare one of the reactants at the appropriate location. In general, this will give a broad range of collision energies, perhaps a few kelvin. In our group, we demonstrated the use of a double-slit chopper to select two different parts of the beam pulse for precise control over the collision energy in intrabeam collisions of Rydberg atoms.[30] Zare and coworkers also have used the intrabeam strategy for inelastic scattering of vibrationally excited D_2 and HD.[31-33] Although in that case the collision energy was not well-defined, the fact that the interaction is dominated by resonances still permits very close comparison with theory.[34, 35] Another approach to achieving low collision energies is to use a low intersection angle for the two molecular beams. This approach has been used by Bergeat et al. with a variable intersection angle apparatus, down to a minimum of 12.5°,

to achieve collision energies down to a few cm^{-1} for both inelastic and reactive collisions with H_2.[36-38] We recently built an instrument that achieves a 4° intersection angle to study cold collisions coupled with velocity map imaging detection.[39] This beam configuration allows fine tuning the collision energy well above room temperature down to the cold regime without any field manipulation. Although trapping and Penning ionization methods can offer access to very low temperatures, scattering experiments that can provide differential cross sections allow close comparison to theory and can reveal novel aspects of the interactions. The velocity map imaging (VMI) technique, readily employed with single-quantum state detection, has allowed measurements of energy dependent state-to-state differential cross sections (DCSs) and integral cross sections (ICSs) while directly revealing underlying the quantum aspects of the scattering event.[40, 41] We have coupled this with stimulated emission pumping (SEP) to prepare NO in arbitrary single quantum states in the $v = 10$ vibrational manifold for scattering studies, exploring some of the questions raised in the opening paragraph.[42-45] The results have been compared to quantum scattering calculations to test the validity of the PESs for the vibrationally excited molecule and to look for resonances and other quantum signatures in the DCSs. This Perspective provides an overview of the results we have obtained for state-to-state inelastic collisions of vibrationally excited NO(v =10) molecules prepared using the SEP technique with Ar and Ne.

Experimental approach

The collision energy between two colliding species in the center-of-mass frame for a scattering experiment with molecular beams is given by

$$E_{col} = \frac{1}{2}\mu\left(v_1^2 + v_2^2 - 2v_1v_2\cos\theta\right)$$

where μ is the reduced mass, v_1 and v_2 are the velocities of the two beams and θ is the beam intersection angle. Slowing down the beams or minimizing the intersection angle of the beams is necessary to lower the collision energy. Slowing down the beams can be achieved with Stark or Zeeman decelerators as mentioned early in the introduction. Here we have used the alternative approach of controlling the beam velocities and minimizing the intersection angle of the beams, permitting very broad tuning of the collision energy from high to very low values. A 3D model of the near-copropagating beam scattering apparatus is shown in Figure 1.[39] In these studies we prepare highly vibrationally excited NO molecules in single quantum states to obtain state-to-state DCSs at broadly tunable collision energies. Previously, only a few studies with DCSs for inelastic collisions of vibrationally excited NO have been reported. DCSs for inelastic collisions of NO(v=5) with Ar were measured by the Houston group using a photoinitiated reaction between O(^{1}D) and N_2O to prepare NO(v=5).[46] Flash heating followed by supersonic expansion was used to prepare NO(v=1) in our group to obtain the DCSs for inelastic collisions with Ar.[47] Unfortunately, these approaches both lead to populating a broad range of initial quantum states, hindering their ability to make a close comparison with theory. Wodtke and co-workers used the SEP technique pioneered by Field and coworkers to prepare vibrationally excited NO for studies of rovibrational relaxation rates and surface scattering dynamics.[42-45] We coupled this powerful SEP technique with VMI detection for

Figure 1 3D model of the near-copropagating beam scattering apparatus.

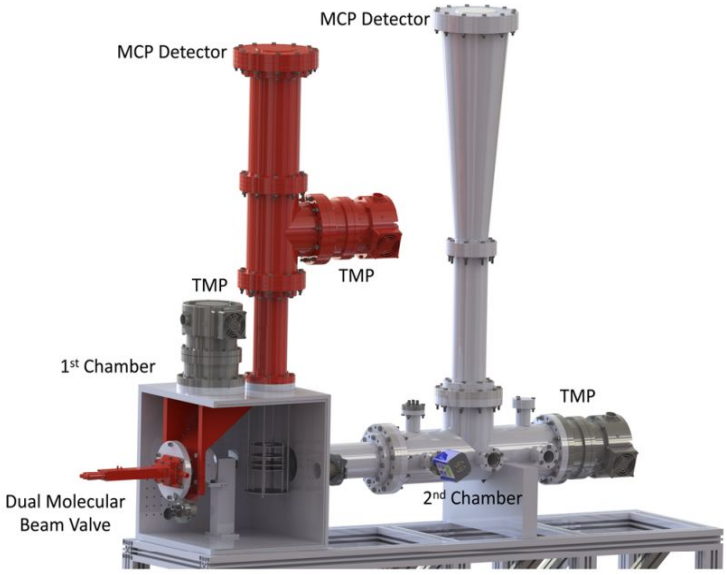

Figure 2. **Schematic of the experimental setup**. Two beams, one containing NO in argon, the other pure argon, are arranged at a 4° intersection angle to collide on the axis of a velocity map imaging spectrometer 32 cm downstream from the nozzles. The NO molecules are prepared in chosen rotational and parity states at the v = 10 level by stimulated emission pumping 1 cm upstream of the collision region. The velocity mapped images of the scattered products are detected in a range of rotational levels of v= 10 via (1 + 1′) resonance-enhanced multiphoton ionization

crossed-beam scattering studies for the first time.

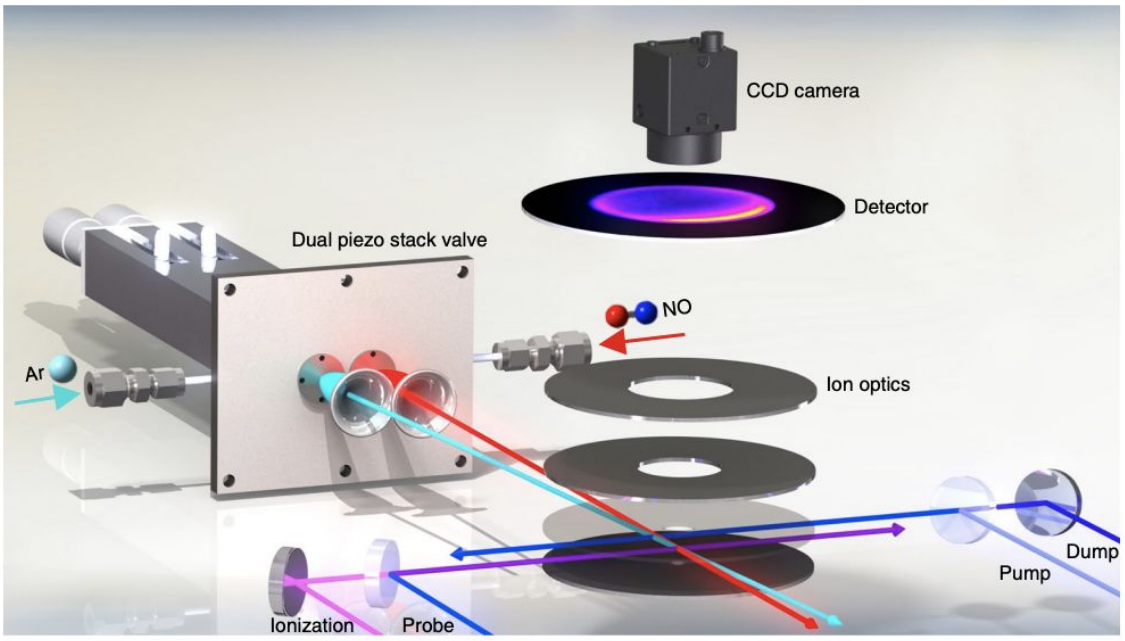

These experiments were carried out in an intrabeam scattering apparatus which was modified to carry out near-copropagating beam scattering.[30, 39, 48] The main addition to the chamber was a dual pulsed valve consisting of two stacked piezo actuators.[49] They are parallel to each other and lie in the same valve body, while the gas inlets and reservoirs are separated from each other. A differential wall is used to reduce the background in the interaction region as well as to aid in achieving single collision conditions. The two molecular beams here are introduced to the same source chamber unlike in a conventional crossed molecular beam method. The primary beam and center skimmer lie on the central axis of the chamber while second skimmer is placed to achieve 4° intersection angle at the interaction region, 32 cm downstream. This low intersection angle allows the fine tuning of the collision energy from well above room temperature down to the cold limit (<1 K). The molecular beams intersect at the middle of repeller and extractor lenses of the DC slice VMI setup and the ionized products are extracted perpendicular to the beam plane. An

imaging microchannel plate detector coupled to a P47 phosphor screen, at a distance of 80 cm from the interaction region, was used to detect the ions.

Preparation of vibrationally excited NO in a single quantum state using SEP is the next key aspect of this set of experiments. A total of four tunable pulsed UV dye lasers were used in this experiment as shown in Figure 2.[50] Two laser beams are used for the SEP state preparation, and two are used for the 1+1' resonant ionization step for detection. The SEP lasers cross the NO molecular beam 1 cm upstream from the interaction region. The SEP preparation schemes used for the studies are shown in Figure 3. The NO molecules were first prepared in the v =10, j=0.5, Ω=0.5, +e state for scattering into a range of final states. Velocity mapped images were acquired over many hours at a repetition rate of 10 Hz and recorded using our own NuAcq image acquisition software and then the DCSs were obtained by the Finite Slice Analysis (FinA) reconstruction software developed in our group.[51, 52] These were then used to extract the underlying DCSs using a Monte Carlo (MC) forward convolution approach for comparison to theory as described further below.

Velocity selection by SEP along with short (~35 μs) molecular beam pulses resulted in excellent speed ratios (v / Δv=45) for the NO beam in the prepared state. As the scattering was not confined

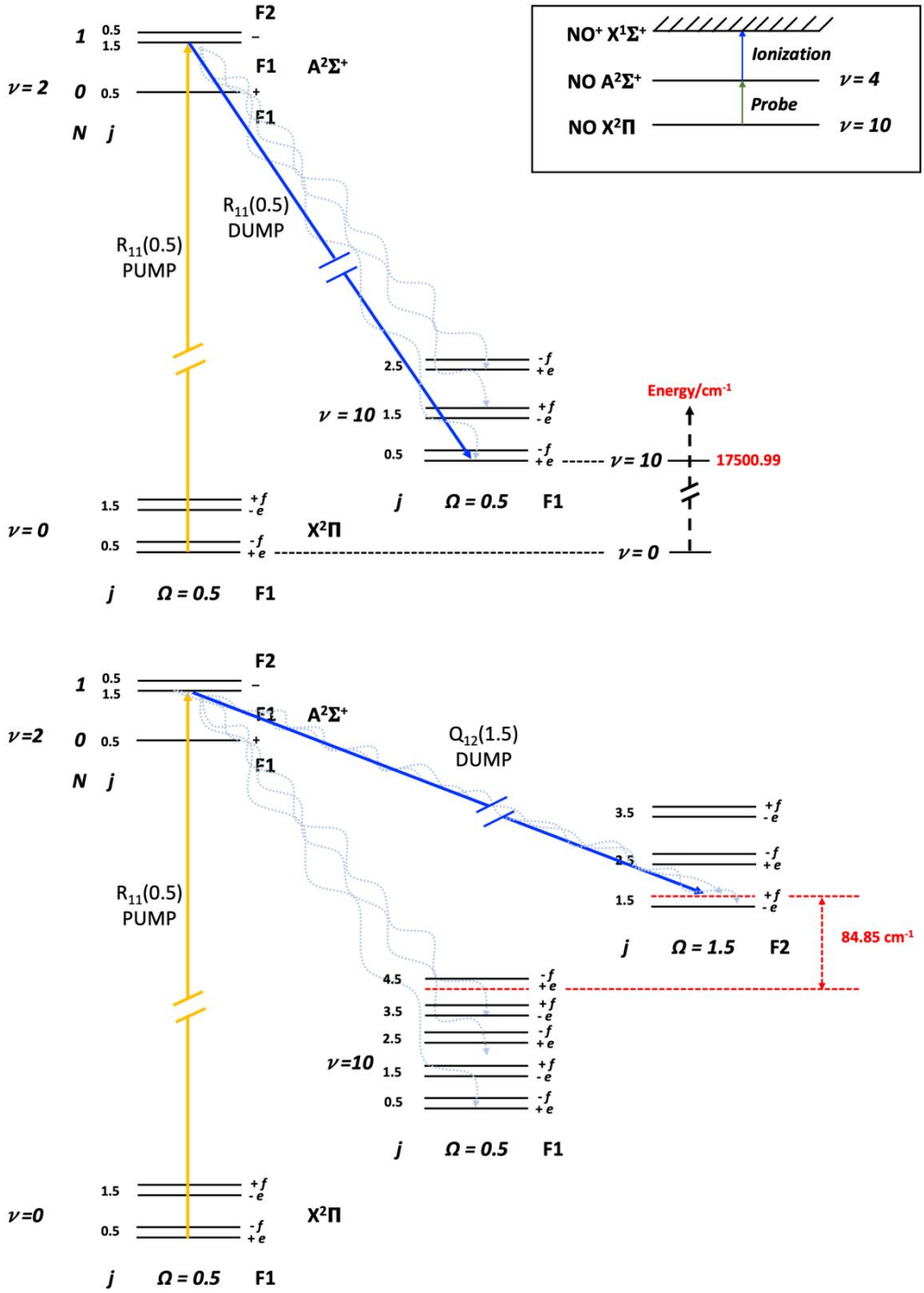

to the probe region, the probe delay was scanned during the experiment to sample over all the

Figure 3. Preparation scheme used to produce (upper panel) NO $X^2\Pi$ ($v = 10$, $\Omega = 0.5$, $j = 0.5$, $+e$) for spin-orbit conserving collisions and (lower panel) NO $X^2\Pi$ ($v = 10$, $\Omega = 1.5$, $j = 1.5$, $+f$) for spin-orbit changing collisions. The solid lines correspond to laser transitions and the curly lines depict spontaneous emission. The inset shows the probe and ionization transitions.

scattered products uniformly. The near-copropagating beam configuration results in a much

smaller density-to-flux correction compared a conventional crossed beam configuration. This is because the range of probed lab velocities is less than a factor of two at most rather than several orders of magnitude as is often the case. This is clearly evident from the near symmetry in the raw experimental images shown in Figure 4. However, there is an enhanced detection sensitivity towards scattered products with larger lab velocities as the detection region is not coincident with the scattering volume. A MC forward convolution simulation was carried out to account for this lab to center-of-mass Jacobian correction and to extract the center-of-mass DCS from the experimental images. Experimental parameters such as velocity, velocity and angular spread of the beams, pump/dump volume and probe volume, interaction volume and time delays of the lasers were included in the simulations.

Theoretical approach

Quantum mechanical characterization of rotationally inelastic scattering of diatomic molecules by atoms has mostly been formulated within the close-coupling framework, in which the Schrödinger equation is solved with the appropriate boundary conditions.[53] This time-independent quantum mechanical close-coupling (QMCC) approach is particularly suitable for cold collisions due to the long de Broglie wavelength.[6] The previous studies of the NO + Rg (e.g., Ar and Ne) scattering have mostly based on the rigid-rotor approximation, which is appropriate for low-lying vibrational states.[53] The highly vibrationally excited NO studied here poses two challenges. First, the potential involvement of the vibrational degree of freedom requires a full-dimensional treatment of the scattering dynamics. Second, the stretched N-O bond length calls for a multi-reference treatment of the electronic structure, as single-reference methods such as coupled cluster fail as the molecule

approaches the dissociation limit. To this end, we have developed a full-dimensional scattering method for scattering of an open-shell molecule by a closed shell atom, in which all the electronic and rotational angular momenta are explicitly included.[54] In addition, PESs were constructed using a multi-reference configuration interaction (MRCI) method,[50] in addition to the gold-standard coupled cluster singles, doubles and perturbative triples (CCSD(T)) method. The details of the ab initio calculations and fitting procedures can be found in our recent publication.[50] For the NO scattering with rare gas atoms, two coupled PESs for the A′ and A″ states are involved, due to the breakdown of the Born-Oppenheimer approximation.

Collision energy dependence of the state-to-state DCS

The SEP technique was used to prepare NO molecules in the $X^2\Pi_{1/2}$ (v = 10, j = 0.5, +e) level,

with the fraction of $v = 10$ NO in the prepared state ~93% for the first set of experiments. The

pump dye laser was set to R_{11} +Q_{21} (0.5) via the 2-0 band of the $A^2\Sigma^+ \leftarrow X^2\Pi$ transition and the

dump laser was set to R_{11} +Q_{21} (0.5) via the 2-10 band of the $A^2\Sigma^+ \rightarrow X^2\Pi$ transition to prepare

the vibrationally excited NO from the SEP scheme. Following the collision with Ar, products

scattered into the NO $X^2\Pi_{1/2}$ ($v = 10, j = 9.5, +f$) level were probed using (1+1') REMPI around

278 nm via the 4-10 band of the $A^2\Sigma^+ \leftarrow X^2\Pi$ transition followed by ionization at the threshold at 327 nm. State-to-state DCSs were recorded from the DC sliced images at four different collision energies, which were obtained using different seed gas compositions of the NO beam. The obtained images are presented in Figure 4 along with the theoretical predictions from QMCC calculations obtained with CCSD(T) PESs.[50] This study was focused on parity-conserving

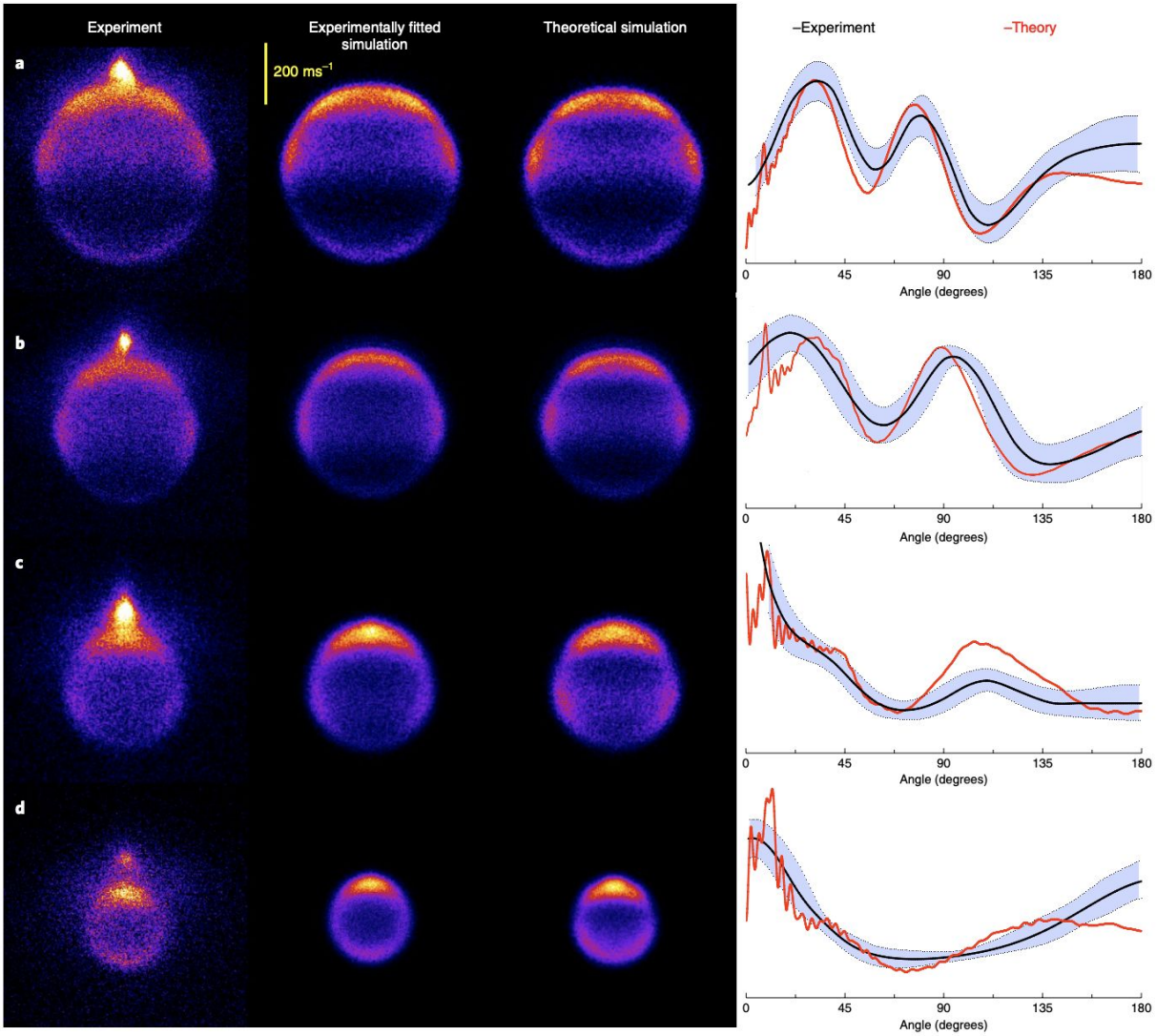

Figure 4. Experimental and simulated images for different collision energies with corresponding DCSs. a–d, The raw experimental DC slice images (first column); simulated, experimentally fitted DCS images (second column); simulated, theoretical DCS images (third column); and experimentally fitted (black) and theoretical (red) DCSs (fourth column) of the inelastic scattering of NO $X^2\Pi_{1/2}$ ($v = 10$, $j = 0.5$, $+e$) with Ar resulting in NO $X^2\ \Pi_{1/2}$ ($v = 10$, $j = 9.5$, $+f$) at 530 ± 40 cm^{-1} (a), 422 ± 40 cm^{-1} (b), 323 ± 32 cm^{-1} (c) and 258 ± 26 cm^{-1} (d) collision energies. The shaded area represents the uncertainty of the experimental fit.

collisions which generally result in more structured DCSs and greater sensitivity to theory. As the collision energy is lowered, sideways and backward scattered peaks shift to larger scattering angles as can readily be seen in the images. The angular divergence of the beams hindered the observation of forward scattered diffraction oscillations predicted in the theoretical DCSs. The sharp intense peaks present in the forward region of the theoretical DCSs are identified as Fraunhofer diffraction oscillations.[55] These are washed out in the first two collision energies but as the width of these features increases as the collision energy decreases, there is some evidence of their existence in the low energy experimental DCSs. We achieved reasonable agreement between experiment and QMCC/CCSD(T) calculations for this part of the experiment. In some cases, such as 323 cm^{-1} in Fig. 4, we see a modest discrepancy. We suspect this could be the result of spontaneous emission populating nearby rotational levels rather than the dumped level.

The repulsive part of the PESs largely governs rotationally inelastic scattering conducted at collision energies corresponding to room temperature or higher. As the bulk of NO-Rg studies to-date have been carried out at such high collision energies, the accuracy of attractive part of the PESs remains relatively untested. The importance of the attractive potential in the current observations can be appraised by comparing the experimental results with a hard-shell model which does not include an attractive component. Quantum interference structures in DCSs and ICSs have been predicted by a simple model originally introduced by McCurdy and Miller and extended by Korsch and Schinke.[56-58] Brouard and co-workers adapted this picture to treat NO-Ar scattering in particular.[59] Scattering phase shifts associated with collisions that are head-on at the N end or O end, or side-on, may be simply estimated and used to predict the interference structures. Approximate positions of the peaks that occur in DCSs for rotationally inelastic collisions for a

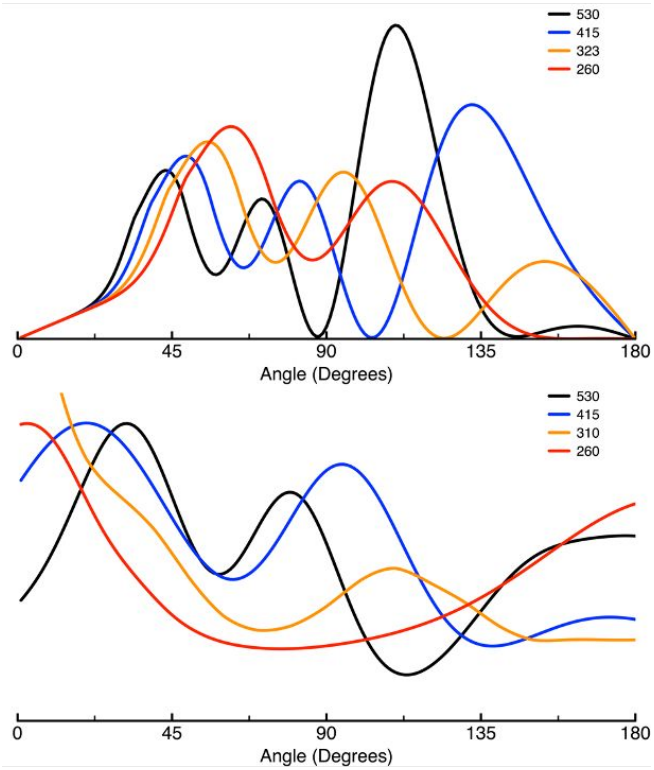

Figure 5. **(Top)** DCSs from the hard-shell model. **(Bottom)** The experimentally fitted DCSs for collisions between NO $X^2\Pi_{1/2}$ ($v = 10$, $j = 0.5$, $+e$) and Ar resulting in NO $X^2\Pi_{1/2}$ ($v = 10$, $j = 9.5$, $+f$) at 530 cm^{-1} (black), 415 cm^{-1} (blue), 323 cm^{-1} (orange) and 260 cm^{-1} (red) collision energies.

hard-shell ellipsoid can then be predicted using the infinite order sudden approximation in the classically allowed region. Figure 5 shows the DCSs obtained for studies we have done involving NO($v = 10$)-Ar collisions at different collision energies using this four-path hard-shell model. As shown in Figure 5, the hard-shell model predicts that when decreasing collision energy, both forward and backward peaks shift to larger scattering angles, consistent with interference terms involving the repulsive potential only. This could be further understood by the need of lower impact parameter collisions to achieve the momentum transfer needed to drive the same rotational excitation when the collision energy is lowered. This is behavior is indeed seen in our experimental results for both sideways and backward scattering. However, the opposite result is seen for forward scattering. This reflects the importance of the attractive part of the PESs for low scattering angles that are classically forbidden.

Varying initial state preparation and control over the final scattering angle

One advantage of using the powerful SEP technique compared to other initial state preparation methods which rely on the Stark effect is the ability to select a range of initial states for scattering.

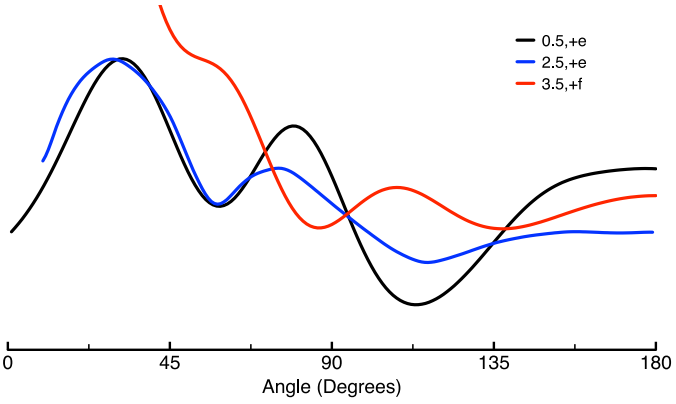

Figure 6. Demonstration of the control over the final scattering angle for collisions into the same final state at the same collision energy by preparing different initial states. Experimentally fitted DCSs for inelastic collisions of NO $X^2\Pi_{1/2}$ ($v = 10$, $j = 0.5$, $+e$) (black), NO $X^2\Pi_{1/2}$ ($v = 10$, $j = 2.5$, $+e$) (blue) and NO $X^2\Pi_{1/2}$ ($v = 10$, $j = 3.5$, $+f$) (red) with Ar resulting in NO $X^2\Pi_{1/2}$ ($v = 10$, $j = 9.5$, $+f$) at a collision energy of 530 cm^{-1}.

This ability can be utilized to study rotational inelastic collisional processes such as rotational de-excitation upon collisions ("superelastic scattering"), and to prepare aligned molecules for stereodynamics studies. This also gives us the ability to control the DCS of the scattered products into the same final state at same collision energy by selecting differing combinations of initial states. This is illustrated for three different initial states of NO: $X^2\Pi_{1/2}$ ($v = 10$, $j = 2.5$, $+e$) and $X^2\Pi_{1/2}$ ($v = 10$, $j = 3.5$, $+f$ and $-e$). In Figure 6, we show the experimental DCSs extracted from the images highlighting these differences. By making varying linear combinations of these or other initial states, one may manipulate and control the final DCS. Despite the extended N-O bond length, the CCSD(T) PESs still shows good agreement with experiment for these spin-orbit conserving collisions.

Rotational de-excitation at low collision energies

The chief advantage of utilizing the near-copropagating beam approach is the ability to reach low collision energies, although the minimal density-to-flux correction mentioned above is also beneficial. Here, we demonstrate another aspect, which is the rotational de-excitation of NO

molecules upon collisions with Ar. As shown in Figure 7, we tuned down to collision energies of 45 cm^{-1} and 32 cm^{-1} with the NO prepared in the $X^2\Pi_{1/2}$ ($v = 10, j = 2.5, +e$) level and the scattered products detected in $X^2\Pi_{1/2}$ ($v = 10, j = 0.5, +e$) level. This allows us to achieve sufficient energy release that we can still obtain an image from which to extract the DCS. The agreement here with the theoretical predictions is quite good.

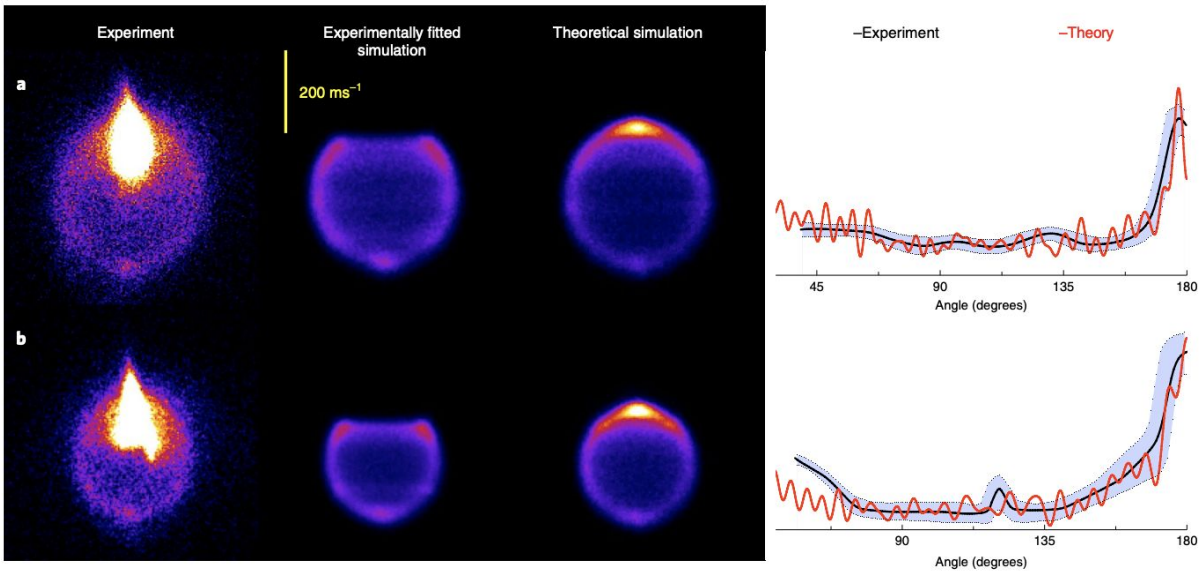

Figure 7. Experimental and simulated images for rotational de-excitation at low collision energies with corresponding DCSs. a,b, The raw experimental d.c. slice images (first column); simulated, experimentally fitted DCS images (second column); simulated, theoretical DCS images (third column); and experimentally fitted (black) and theoretical (red) DCSs (fourth column) for inelastic scattering of NO $X^2\Pi_{1/2}$ ($v = 10$, j= 2.5, $+e$) with Ar resulting in NO $X^2\Pi_{1/2}$ (v= 10, j= 0.5, $+e$) at collision energies of 48 ± 8 cm^{-1} (a) and 32 ± 6 cm^{-1} (b). The forward scattering has been omitted from the simulation owing to interfering background. The shaded area represents the uncertainty of the experimental fit.

State-to-state spin-orbit changing collisions of NO (v = 10) down to 2 K

Taking a further step of this strategy of converting the reactant internal energy to translational energy, by preparing NO initially in a spin-orbit excited state and monitoring the ground state, we were able to reach the cold regime near 2 K and still obtain high quality DCSs. In this case we

prepare spin-orbit excited NO $X^2\Pi$ (v = 10, Ω=1.5, j = 1.5) using the SEP scheme in the lower panel of Figure 2 and probe the ground spin-orbit state following collision with Ar and Ne.[60, 61] These results were compared with QMCC calculations done with CCSD(T) and MRCI PESs. As shown above, QMCC scattering calculations have been quite successful in reproducing the essential features in the experimental results for these spin-orbit conserving processes using CCSD(T) PESs. These studies involving cold, spin-orbit changing collisions allow us to test the accuracy of the attractive part of the difference potential for both NO-Ar and NO-Ne systems which was untested earlier. Furthermore, the scattering is largely governed by resonances in this collision energy regime providing a stringent test for theory. Even though NO was prepared in NO $X^2\Pi$ (v = 10, Ω=1.5, j = 1.5, +f), weak fields in our set up are believed to be mix the parity levels which in this case are only separated by 0.6 MHz.[62]

Having the ability to pick a subset of velocities from the velocity spread of the NO beam using the SEP technique enabled us to fine tune the collision energy from 1.5 cm^{-1} to 3.5 cm^{-1} (~2-5 K) with much improved energy resolution. This can be seen in figure 8 from the change of the direction of relative velocity in response to subtle changes of the velocity, clearly demonstrating our ability to fine tune the collision energy by utilizing SEP at different time delays. Inelastic scattering of NO molecules from the $X^2\Pi$ (v = 10, Ω=1.5, j = 1.5) level to $X^2\Pi$ (v = 10, Ω=0.5, j = 4.5, +e) state results in an excess energy of 84.9 cm^{-1}.

The images show strong scattering towards the forward direction and enhanced scattering towards backward direction as well. Many scattering experiments involving NO lose information on the forward direction due to interference by non-resonant ionization of the beam. This is not an issue

here due to notable velocity difference between the beam NO and scattered NO. Figure 9 shows

the comparison of experimental results with QMCC calculations. The images have been rotated so

that the relative velocity vector is vertical and forward scattering in upward, allowing a simple

comparison. The DCSs extracted from the MC forward convolution simulations were compared

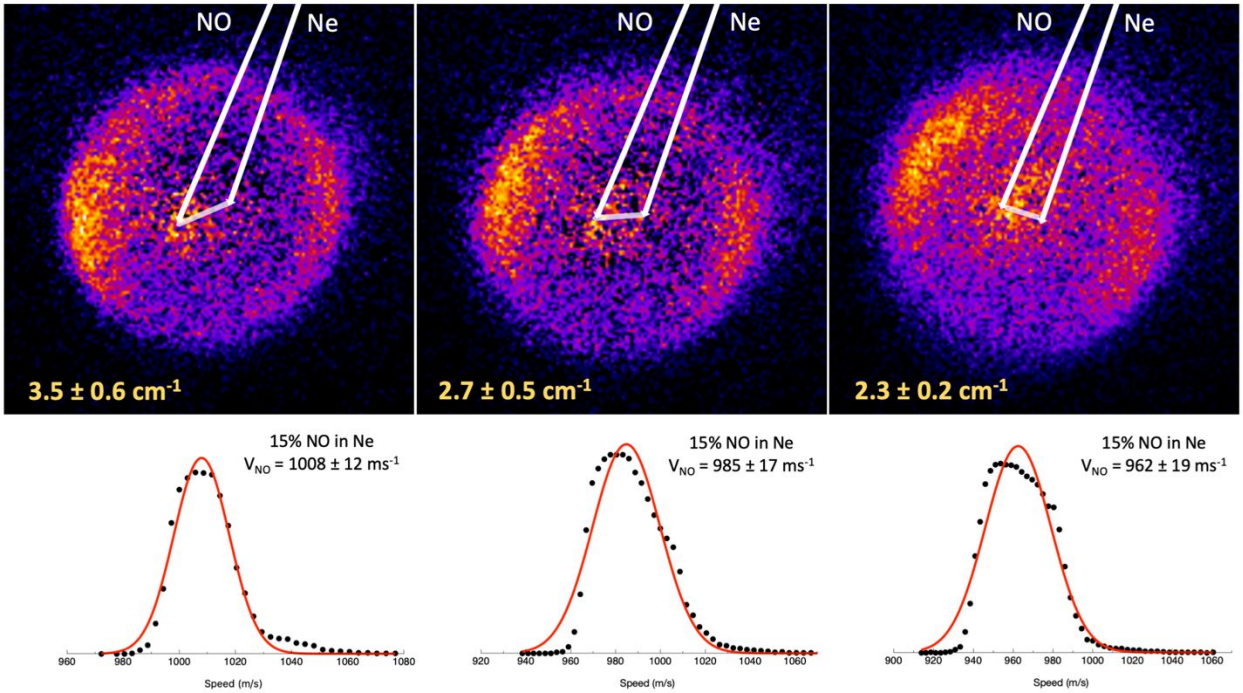

Figure 8. (Top) Background-subtracted raw experimental images for NO $X^2\Pi$ (v = 10, Ω'' = 1.5, j'' = 1.5) + Ne → NO $X^2\Pi$ (v = 10, Ω' = 0.5, j' = 4.5, +e) + Ne at (left) 3.5 cm^{-1}, (middle) 2.7 cm^{-1} and (right) 2.3 cm^{-1} collision energies. (Bottom) The velocity distributions of corresponding NO $X^2\Pi$ (v = 10, Ω'' = 1.5, j'' = 1.5) obtained by neutral time-of-flight measurements.

with the corresponding DCSs obtained from QMCC calculations done for NO(v = 10)-Ne spin-

orbit changing collisions using an RCCSD(T)/ aug-cc-pVTZ level PES. The MC simulations

successfully reproduced the features present in the raw images including the asymmetry seen in

the images. This further confirms that the MC simulation embodies all the key elements in the

experiment. This asymmetry was due to the detection bias towards some lab velocities over the

other which we minimized by scanning the time delay between SEP lasers and probe laser delay.

A good agreement was observed between experiment and theory for all three collision energies for

spin-orbit changing NO-Ne collisions. However, for NO-Ar spin-orbit changing collisions, there

were clear disagreements between experimental and theoretical DCSs from the CCSD(T) PESs.[60]

This was more evident at 3.5 cm^{-1} collision energy where theoretical DCSs from scattering

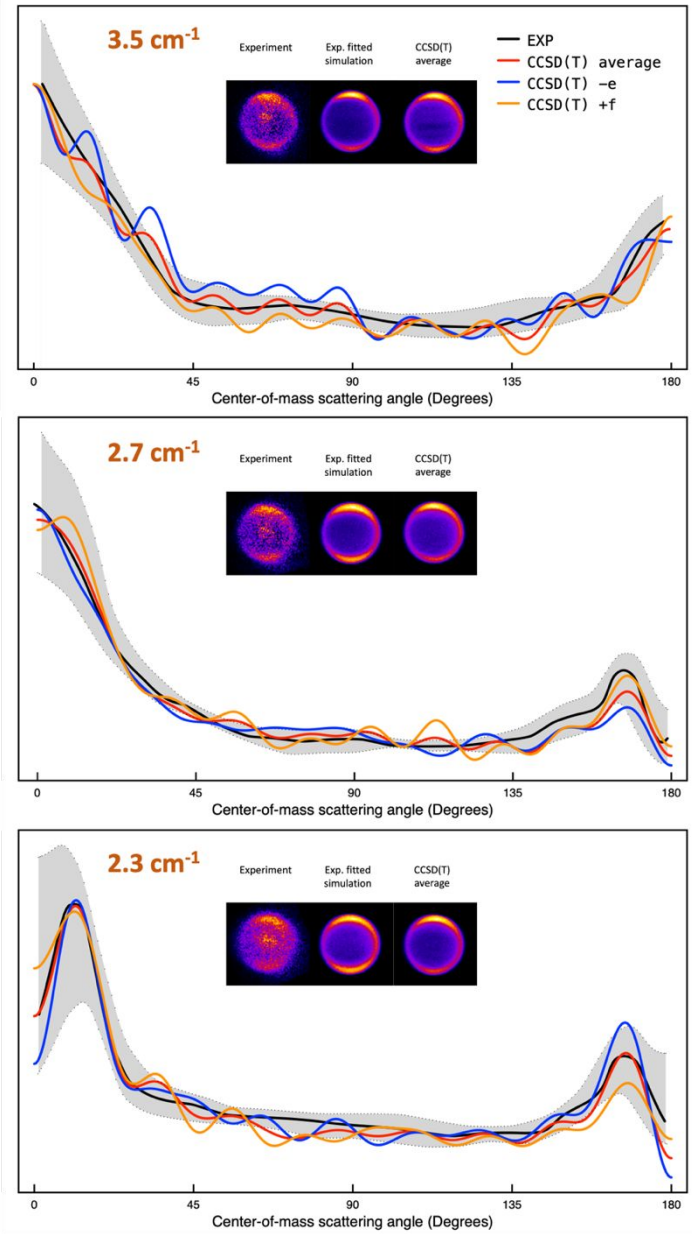

Figure 9. Experimental and simulated images for different collision energies with corresponding DCSs. Experimentally fitted (black) and 3D QMCC predicted with an incoherent sum of initial parities (red), initial parity '*e*' (blue), and initial parity "*f*" (orange) DCSs for NO $X^2\Pi$ ($v = 10$, $\Omega'' = 1.5$, $j'' = 1.5$) + Ne → NO $X^2\Pi$ ($v = 10$, $\Omega' = 0.5$, $j' = 4.5$, +*e*) + Ne at (top) 3.5 cm^{-1}, (middle) 2.7 cm^{-1}, and (bottom) 2.3 cm^{-1} collision energies. The inset shows (left) the raw experimental image without background, (middle) Monte Carlo simulated experimentally fitted DCS image, and (right) CCSD(T)-predicted image for an average of initial parities. The shaded area represents the uncertainty of the experimental fit estimated by adjusting the intensity at a range of selected angles until the squared residuals increased more than 10%. The images are rotated so that the relative velocity vector is vertical and the forward scattering direction is upward.

calculations done on an MRCI PESs agreed somewhat better, particularly in the forward direction.

The better agreement for the MRCI PESs may be fortuitous, as the CCDS(T) PESs is likely to be

more accurate overall. However, the dynamics at this low energy are dominated by resonances, and the MRCI PESs may happen to catch the features of the potential responsible. Furthermore, overall, the NO-Ar PESs are not as precise as the NO-Ne PESs due to the larger number of electrons. This, combined with the sensitivity of these spin-orbit changing collisions to the difference potential, with inherently larger relative error, may account for the greater discrepancies of the NO-Ar spin-orbit changing calculations.

One notable feature of the lowest collision energy result is the appearance of enhanced backward scattering, well captured by the theory. To gain insight into its origin, we have performed a partial

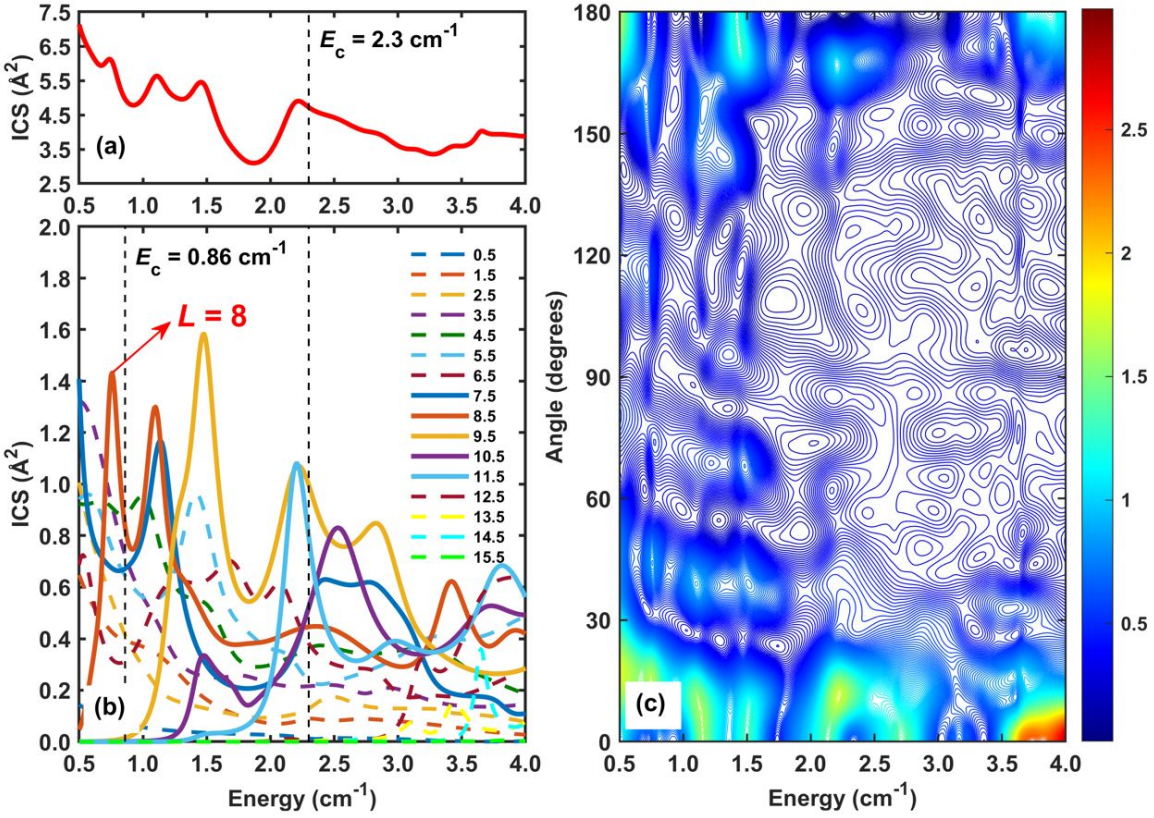

Figure 10. Collisional energy dependence of the ICSs (left top) and DCSs (right) for the NO $X^2\Pi$ (v = 10, Ω'' = 1.5, j'' = 1.5) + Ne → NO $X^2\Pi$ (v = 10, Ω' = 0.5, j' = 4.5, +e) + Ne process at the collision energy range from 0.5 to 4 cm^{-1} with an energy grid of 0.01 cm^{-1}. (Left bottom) A partial wave analysis suggests that the peak at 2.3 cm^{-1} is due to several overlapping resonances.

wave analysis, shown in Figure 10. The partial wave analysis shows evidence of overlapping resonances that are attributed to quasi-bound NO-Ne levels near 2.3 cm^{-1}. These contributions are from partial waves with total angular momentum J=7.5 to 11.5, dominated by J=9.5 and 11.5. These give rise to a broad bump in the ICS due to overlapping resonances and the enhanced backscattering seen in the results. To identify isolated resonances in this system we would have to go to much lower collision energies that we have access to at present.

Conclusions and outlook

These studies show the versatility of the combination of the near-copropagating beam technique with SEP and velocity map imaging. We have obtained DCSs for rotationally inelastic collisions of translationally cold NO (< 5 K) while carrying vibrational excitation of ~2 eV. We have shown the preparation of single ro-vibrational and parity levels for state-to-state scattering in both spin-orbit manifolds of NO. Control over the DCSs using different initial states was illustrated utilizing the flexibility of the SEP technique. The attractive part of the PESs were probed using the broad tunability of the collision energy owing to near-copropagating beam configuration. The experimental results showed overall good agreement with QMCC calculations done on both CCSD(T) and MRCI PESs even at these challenging and rather extreme experimental conditions. Collisions of vibrationally excited NO molecules are not limited to studies of rotationally inelastic collisions. Vibrational inelastic collisions might play a significant role if NO molecules are excited to much higher vibrational levels where rotational and vibrational spacing approach each other. This can open novel pathways while presenting key challenges to coupled-cluster methods. Extending these approaches to scattering of triatomic and polyatomic molecules and to lower

collision energies using intrabeam methods should afford new insights into molecular dynamics in this quantum realm.

Acknowledgments

This work was supported by the ARO under MURI award W911-NF-19-0238.

References

(1) Heazlewood, B. R.; Softley, T. P. Towards Chemistry at Absolute Zero. *Nature Reviews Chemistry* **2021**, *5* (2), 125-140.

(2) Margulis, B.; Narevicius, J.; Narevicius, E. Direct Observation of a Feshbach Resonance by Coincidence Detection of Ions and Electrons in Penning Ionization Collisions. *Nature Communications* **2020**, *11* (1), 3553.

(3) de Jongh, T.; Shuai, Q.; Abma, G. L.; Kuijpers, S.; Besemer, M.; van der Avoird, A.; Groenenboom, G. C.; van de Meerakker, S. Y. T. Mapping Partial Wave Dynamics in Scattering Resonances by Rotational de-Excitation Collisions. *Nature Chemistry* **2022**, *14* (5), 538-544.

(4) de Jongh, T.; Besemer, M.; Shuai, Q.; Karman, T.; van der Avoird, A.; Groenenboom, G. C.; van de Meerakker, S. Y. T. Imaging the Onset of the Resonance Regime in Low-Energy NO-He Collisions. *Science* **2020**, *368* (6491), 626-630.

(5) Bohn, J. L.; Rey, A. M.; Ye, J. Cold Molecules: Progress in Quantum Engineering of Chemistry and Quantum Matter. *Science* **2017**, *357* (6355), 1002-1010.

(6) Balakrishnan, N. Perspective: Ultracold Molecules and the Dawn of Cold Controlled Chemistry. *The Journal of chemical physics* **2016**, *145* (15), 150901.

(7) Quéméner, G.; Julienne, P. S. Ultracold Molecules under Control. *Chemical Reviews* **2012**, *112* (9), 4949-5011.

(8) Krems, R.; Friedrich, B.; Stwalley, W. C. *Cold Molecules: Theory, Experiment, Applications*; CRC press, 2009.

(9) Ospelkaus, S.; Ni, K.-K.; Wang, D.; De Miranda, M.; Neyenhuis, B.; Quéméner, G.; Julienne, P.; Bohn, J.; Jin, D.; Ye, J. Quantum-State Controlled Chemical Reactions of Ultracold Potassium-Rubidium Molecules. *Science* **2010**, *327* (5967), 853-857.

(10) Ni, K.-K.; Ospelkaus, S.; Wang, D.; Quéméner, G.; Neyenhuis, B.; De Miranda, M.; Bohn, J.; Ye, J.; Jin, D. Dipolar Collisions of Polar Molecules in the Quantum Regime. *Nature* **2010**, *464* (7293), 1324-1328.

(11) De Marco, L.; Valtolina, G.; Matsuda, K.; Tobias, W. G.; Covey, J. P.; Ye, J. A Degenerate Fermi Gas of Polar Molecules. *Science* **2019**, *363* (6429), 853-856.

(12) Matsuda, K.; De Marco, L.; Li, J.-R.; Tobias, W. G.; Valtolina, G.; Quéméner, G.; Ye, J. Resonant Collisional Shielding of Reactive Molecules Using Electric Fields. *Science* **2020**, *370* (6522), 1324-1327.

(13) van de Meerakker, S. Y.; Bethlem, H. L.; Vanhaecke, N.; Meijer, G. Manipulation and Control of Molecular Beams. *Chemical Reviews* **2012**, *112* (9), 4828-4878.

(14) Hutzler, N. R.; Lu, H.-I.; Doyle, J. M. The Buffer Gas Beam: An Intense, Cold, and Slow Source for Atoms and Molecules. *Chemical Reviews* **2012**, *112* (9), 4803-4827.

(15) Wu, X.; Gantner, T.; Koller, M.; Zeppenfeld, M.; Chervenkov, S.; Rempe, G. A Cryofuge for Cold-Collision Experiments with Slow Polar Molecules. *Science* **2017**, *358* (6363), 645-648.

(16) Segev, Y.; Pitzer, M.; Karpov, M.; Akerman, N.; Narevicius, J.; Narevicius, E. Collisions between Cold Molecules in a Superconducting Magnetic Trap. *Nature* **2019**, *572* (7768), 189-193.

(17) Koller, M.; Jung, F.; Phrompao, J.; Zeppenfeld, M.; Rabey, I.; Rempe, G. Electric-Field-Controlled Cold Dipolar Collisions between Trapped CH_3F Molecules. *Physical Review Letters* **2022**, *128* (20), 203401.

(18) Stuhl, B. K.; Hummon, M. T.; Yeo, M.; Quéméner, G.; Bohn, J. L.; Ye, J. Evaporative Cooling of the Dipolar Hydroxyl Radical. *Nature* **2012**, *492* (7429), 396-400.

(19) Son, H.; Park, J. J.; Ketterle, W.; Jamison, A. O. Collisional Cooling of Ultracold Molecules. *Nature* **2020**, *580* (7802), 197-200.

(20) Suits, A. G.; Bontuyan, L. S.; Houston, P. L.; Whitaker, B. J. Differential Cross Sections for State-Selected Products by Direct Imaging: Ar+NO. *The Journal of Chemical Physics* **1992**, *96* (11), 8618-8620.

(21) Bontuyan, L. S.; Suits, A. G.; Houston, P. L.; Whitaker, B. J. State-Resolved Differential Cross Sections for Crossed-Beam Argon-Nitric Oxide Inelastic Scattering by Direct Ion Imaging. *The Journal of Physical Chemistry* **1993**, *97* (24), 6342-6350.

(22) Vogels, S. N.; Onvlee, J.; Chefdeville, S.; van der Avoird, A.; Groenenboom, G. C.; van de Meerakker, S. Y. Imaging Resonances in Low-Energy NO-He Inelastic Collisions. *Science* **2015**, *350* (6262), 787-790.

(23) Von Zastrow, A.; Onvlee, J.; Vogels, S. N.; Groenenboom, G. C.; Van Der Avoird, A.; Van De Meerakker, S. Y. State-Resolved Diffraction Oscillations Imaged for Inelastic Collisions of NO Radicals with He, Ne and Ar. *Nature chemistry* **2014**, *6* (3), 216-221.

(24) Kirste, M.; Wang, X.; Schewe, H. C.; Meijer, G.; Liu, K.; van der Avoird, A.; Janssen, L. M.; Gubbels, K. B.; Groenenboom, G. C.; van de Meerakker, S. Y. Quantum-State Resolved

Bimolecular Collisions of Velocity-Controlled OH with NO Radicals. *Science* **2012**, *338* (6110), 1060-1063.

(25) Tang, G.; Besemer, M.; Kuijpers, S.; Groenenboom, G. C.; van der Avoird, A.; Karman, T.; van de Meerakker, S. Y. Quantum State–Resolved Molecular Dipolar Collisions over Four Decades of Energy. *Science* **2023**, *379* (6636), 1031-1036.

(26) Henson, A. B.; Gersten, S.; Shagam, Y.; Narevicius, J.; Narevicius, E. Observation of Resonances in Penning Ionization Reactions at Sub-Kelvin Temperatures in Merged Beams. *Science* **2012**, *338* (6104), 234-238.

(27) Jankunas, J.; Bertsche, B.; Osterwalder, A. Study of the Ne ($^3P_2$)+ CH_3F Electron-Transfer Reaction Below 1 K. *The Journal of Physical Chemistry A* **2014**, *118* (22), 3875-3879.

(28) Shagam, Y.; Klein, A.; Skomorowski, W.; Yun, R.; Averbukh, V.; Koch, C. P.; Narevicius, E. Molecular Hydrogen Interacts More Strongly When Rotationally Excited at Low Temperatures Leading to Faster Reactions. *Nature Chemistry* **2015**, *7* (11), 921-926.

(29) Gordon, S. D.; Omiste, J. J.; Zou, J.; Tanteri, S.; Brumer, P.; Osterwalder, A. Quantum-State-Controlled Channel Branching in Cold Ne ($^3P_2$)+ Ar Chemi-Ionization. *Nature Chemistry* **2018**, *10* (12), 1190-1195.

(30) Amarasinghe, C.; Suits, A. G. Intrabeam Scattering for Ultracold Collisions. *The Journal of Physical Chemistry Letters* **2017**, *8* (20), 5153-5159.

(31) Perreault, W. E.; Mukherjee, N.; Zare, R. N. Cold Quantum-Controlled Rotationally Inelastic Scattering of HD with H_2 and D_2 Reveals Collisional Partner Reorientation. *Nature Chemistry* **2018**, *10* (5), 561-567.

(32) Zhou, H.; Perreault, W. E.; Mukherjee, N.; Zare, R. N. Quantum Mechanical Double Slit for Molecular Scattering. *Science* **2021**, *374* (6570), 960-964.

(33) Zhou, H.; Perreault, W. E.; Mukherjee, N.; Zare, R. N. Anisotropic Dynamics of Resonant Scattering between a Pair of Cold Aligned Diatoms. *Nature Chemistry* **2022**, *14* (6), 658-663.

(34) Jambrina, P. G.; Croft, J. F.; Guo, H.; Brouard, M.; Balakrishnan, N.; Aoiz, F. J. Stereodynamical Control of a Quantum Scattering Resonance in Cold Molecular Collisions. *Physical Review Letters* **2019**, *123* (4), 043401.

(35) Jambrina, P. G.; Croft, J. F.; Zuo, J.; Guo, H.; Balakrishnan, N.; Aoiz, F. J. Stereodynamical Control of Cold Collisions between Two Aligned D_2 Molecules. *Physical Review Letters* **2023**, *130* (3), 033002.

(36) Chefdeville, S.; Stoecklin, T.; Bergeat, A.; Hickson, K. M.; Naulin, C.; Costes, M. Appearance of Low Energy Resonances in CO–Para-H_2 Inelastic Collisions. *Physical Review Letters* **2012**, *109* (2), 023201.

(37) Bergeat, A.; Onvlee, J.; Naulin, C.; Van Der Avoird, A.; Costes, M. Quantum Dynamical Resonances in Low-Energy CO (J= 0)+ He Inelastic Collisions. *Nature Chemistry* **2015**, *7* (4), 349-353.

(38) Chefdeville, S.; Kalugina, Y.; van de Meerakker, S. Y.; Naulin, C.; Lique, F.; Costes, M. Observation of Partial Wave Resonances in Low-Energy O_2–H_2 Inelastic Collisions. *Science* **2013**, *341* (6150), 1094-1096.

(39) Amarasinghe, C.; Perera, C. A.; Suits, A. G. A Versatile Molecular Beam Apparatus for Cold/Ultracold Collisions. *The Journal of Chemical Physics* **2020**, *152* (18), 184201.

(40) Townsend, D.; Minitti, M. P.; Suits, A. G. Direct Current Slice Imaging. *Review of Scientific Instruments* **2003**, *74* (4), 2530-2539.

(41) Eppink, A. T. J. B.; Parker, D. H. Velocity Map Imaging of Ions and Electrons Using Electrostatic Lenses: Application in Photoelectron and Photofragment Ion Imaging of Molecular Oxygen. *Review of Scientific Instruments* **1997**, *68* (9), 3477-3484.

(42) Yang, X.; Wodtke, A. M. Efficient State-Specific Preparation of Highly Vibrationally Excited NO($X^2\Pi$). *The Journal of Chemical Physics* **1990**, *92* (1), 116-120.

(43) Yang, X.; Kim, E. H.; Wodtke, A. M. Vibrational Energy Transfer of Very Highly Vibrationally Excited NO. *The Journal of Chemical Physics* **1992**, *96* (7), 5111-5122.

(44) Silva, M.; Jongma, R.; Field, R. W.; Wodtke, A. M. The Dynamics of "Stretched Molecules": Experimental Studies of Highly Vibrationally Excited Molecules with Stimulated Emission Pumping. *Annual Review of Physical Chemistry* **2001**, *52* (1), 811-852.

(45) C E Hamilton; J L Kinsey, a.; Field, R. W. Stimulated Emission Pumping: New Methods in Spectroscopy and Molecular Dynamics. *Annual Review of Physical Chemistry* **1986**, *37* (1), 493-524.

(46) Dixit, A. A.; Pisano, P. J.; Houston, P. L. Differential Cross Section for Rotationally Inelastic Scattering of Vibrationally Excited NO(v=5) from Ar. *The Journal of Physical Chemistry A* **2001**, *105* (50), 11165-11170.

(47) Kamasah, A.; Li, H.; Onvlee, J.; van der Avoird, A.; Parker, D. H.; Suits, A. G. Imaging the Inelastic Scattering of Vibrationally Excited NO(v = 1) with Ar. *Chemical Physics Letters* **2018**, *692*, 124-128.

(48) Amarasinghe, C.; Li, H.; Perera, C. A.; Besemer, M.; van der Avoird, A.; Groenenboom, G. C.; Xie, C.; Guo, H.; Suits, A. G. Differential Cross Sections for State-to-State Collisions of NO(v = 10) in near-Copropagating Beams. *The Journal of Physical Chemistry Letters* **2019**, *10* (10), 2422-2427.

(49) Abeysekera, C.; Joalland, B.; Shi, Y.; Kamasah, A.; Oldham, J. M.; Suits, A. G. Note: A Short-Pulse High-Intensity Molecular Beam Valve Based on a Piezoelectric Stack Actuator. *Review of Scientific Instruments* **2014**, *85* (11), 116107.

(50) Amarasinghe, C.; Li, H.; Perera, C. A.; Besemer, M.; Zuo, J.; Xie, C.; van der Avoird, A.; Groenenboom, G. C.; Guo, H.; Kłos, J.; et al. State-to-State Scattering of Highly Vibrationally Excited NO at Broadly Tunable Energies. *Nature Chemistry* **2020**, *12* (6), 528-534.

(51) Thompson, J. O. F.; Amarasinghe, C.; Foley, C. D.; Rombes, N.; Gao, Z.; Vogels, S. N.; Meerakker, S. Y. T. v. d.; Suits, A. G. Finite Slice Analysis (FinA) of Sliced and Velocity Mapped Images on a Cartesian Grid. *The Journal of Chemical Physics* **2017**, *147* (7), 074201.

(52) Thompson, J. O. F.; Amarasinghe, C.; Foley, C. D.; Suits, A. G. Finite Slice Analysis (FinA)—a General Reconstruction Method for Velocity Mapped and Time-Sliced Ion Imaging. *The Journal of Chemical Physics* **2017**, *147* (1), 013913.

(53) Alexander, M. H. Rotationally Inelastic Collisions between a Diatomic Molecule in $a^2\Pi$ Electronic State and a Structureless Target. *The Journal of Chemical Physics* **1982**, *76* (12), 5974-5988.

(54) Zuo, J.; Guo, H. Time-Independent Quantum Theory on Vibrational Inelastic Scattering between Atoms and Open-Shell Diatomic Molecules: Applications to NO+ Ar and NO+ H Scattering. *The Journal of Chemical Physics* **2020**, *153* (14).

(55) Onvlee, J.; Gordon, S. D. S.; Vogels, S. N.; Auth, T.; Karman, T.; Nichols, B.; van der Avoird, A.; Groenenboom, G. C.; Brouard, M.; van de Meerakker, S. Y. T. Imaging Quantum Stereodynamics through Fraunhofer Scattering of NO Radicals with Rare-Gas Atoms. *Nature Chemistry* **2017**, *9* (3), 226-233.

(56) McCurdy, C. W.; Miller, W. H. Interference Effects in Rotational State Distributions: Propensity and Inverse Propensity. *The Journal of Chemical Physics* **1977**, *67* (2), 463-468.

(57) Korsch, H. J.; Schinke, R. A Uniform Semiclassical Sudden Approximation for Rotationally Inelastic Scattering. *The Journal of Chemical Physics* **1980**, *73* (3), 1222-1232.

(58) Korsch, H. J.; Schinke, R. Rotational Rainbows: An IOS Study of Rotational Excitation of Hard-Shell Molecules. *The Journal of Chemical Physics* **1981**, *75* (8), 3850-3859.

(59) Eyles, C. J.; Brouard, M.; Yang, C. H.; Kłos, J.; Aoiz, F. J.; Gijsbertsen, A.; Wiskerke, A. E.; Stolte, S. Interference Structures in the Differential Cross-Sections for Inelastic Scattering of NO by Ar. *Nature Chemistry* **2011**, *3* (8), 597-602.

(60) Amarasinghe, C.; Perera, C. A.; Li, H.; Zuo, J.; Besemer, M.; van der Avoird, A.; Groenenboom, G. C.; Guo, H.; Suits, A. G. Collision-Induced Spin-Orbit Relaxation of Highly Vibrationally Excited NO near 1 K. *Natural Sciences* **2022**, *2* (1), e20210074.

(61) Perera, C. A.; Zuo, J.; Guo, H.; Suits, A. G. Differential Cross Sections for Cold, State-to-State Spin–Orbit Changing Collisions of NO(v = 10) with Neon. *The Journal of Physical Chemistry A* **2022**, *126* (21), 3338-3346.

(62) Chen, J.; Matsiev, D.; White, J. D.; Murphy, M.; Wodtke, A. M. Hexapole Transport and Focusing of Vibrationally Excited NO Molecules Prepared by Optical Pumping. *Chemical Physics* **2004**, *301* (2), 161-172.

TOC